A NEW HETERODYNE INTERFREOMETER WITH ZERO PERIODIC ERROR AND TUNABLE BEAT FREQUENCY

Hyo Soo Kim[1], Tony L. Schmitz,[1] John F. Beckwith[2,*], and Matthew C. Rueff[1]
[1]Department of Mechanical and Aerospace Engineering
University of Florida, Gainesville, FL, USA
[2]Electronics Engineering Technologies Division
Lawrence Livermore National Laboratory, Livermore, CA 94550, USA
[*]Retired

INTRODUCTION

Since its introduction in the mid-1960s, displacement measuring interferometry has offered high accuracy, range, and resolution for non-contact displacement measurement applications, including position feedback for lithographic stepper stages, precision cutting machines, and coordinate measuring machines, as well as transducer calibration, for example. A common configuration choice in these situations is the heterodyne (or two frequency) Michelson-type interferometer with single, double, or multiple passes of the optical paths. These systems infer changes in displacement of a selected optical path by monitoring the optically induced variation in the photodetector current, which is generated from the optical interference signal.

Periodic error remains an intrinsic error source that prevents traditional configurations from achieving sub-nanometer level accuracy. The purpose of this research is to validate the absence of periodic error in a new interferometer design that does not rely on polarization coding, where the two (heterodyne) optical frequencies are carried on coincident, linearly polarized, mutually orthogonal laser beams and separated/recombined using polarization dependent optics. Rather, the two frequencies are carried on spatially separate beams in a polarization independent optical configuration that also enables the user to select the beat (or split) frequency. By eliminating the potential for mixing between the two heterodyne frequencies, the periodic error source is removed.

PERIODIC ERROR BACKGROUND

Imperfect separation of the two light frequencies into the moving and fixed paths in polarization coded heterodyne interferometers has been shown to produce first and second order periodic errors, or errors of one and two cycles per wavelength of optical path change, respectively. In a perfect system, a single frequency would travel to the fixed target, while a second, single frequency traveled to the moving target. Interference of the combined signals would yield a perfectly sinusoidal trace with phase that varied, relative to a reference phase signal, in response to motion of the moving target. However, the inherent frequency leakage in actual implementations produces an interference signal which is not purely sinusoidal (i.e., contains unintended spectral content) and leads to a periodic error in the measured displacement.

Quenelle [1] performed an early investigation of periodic error in heterodyne interferometers. Subsequent areas of research have included efforts to measure periodic error using frequency domain analysis [2], analytical modeling techniques [3], Jones calculus modeling [4], and reduction of periodic error [5-7].

Schmitz and Beckwith [8] summarized the potential periodic error contributors using a Frequency-Path model, which identified all possible paths for each light frequency from the source to detector and predicted the number of interference terms that may be expected at the detector output. For the single pass, polarization-coded heterodyne interferometer, it was demonstrated that 10 distinct interference terms exist in a fully leaking interferometer (i.e., each frequency is present in both the moving and fixed paths). These interference terms may be grouped by optical path change dependency into only four categories: 1) o*ptical power* which contributes a constant intensity to the photodetector current independent of optical path changes; 2) *AC reference* terms with phase that varies by one full cycle over the synthetic wavelength; 3) *DC interference*, which are Doppler shifted up from zero frequency during

target motion; and 4) *AC interference* terms which produce a time harmonic variation in the detector current at the beat frequency (f_b) and are Doppler shifted (f_d) up or down during target motion depending on direction. The corresponding frequency content during constant velocity motion is depicted in Fig. 1.

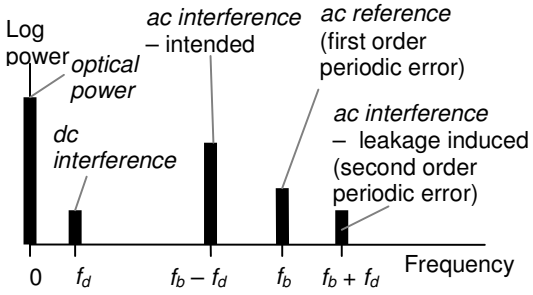

FIGURE 1. Frequency spectrum for constant velocity motion in fully leaking heterodyne interferometer.

EXPERIMENTAL SETUP

In the AOM DMI design, a pair of AOMs is used to generate, and keep spatially separate, the heterodyne frequencies. The basic elements of an AOM are a glass body with a piezoelectric transducer (PZT) attached at one end and a frequency source (stable quartz oscillator) to drive the PZT.

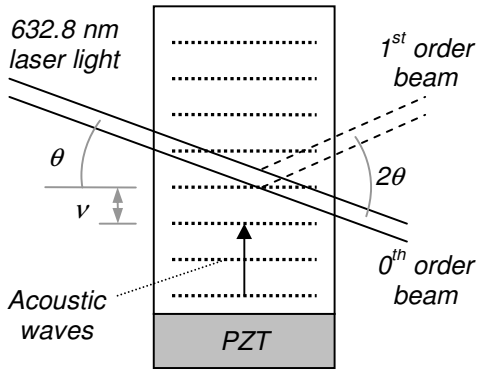

FIGURE 2. Acousto-optic modulator schematic. The incident beam is diffracted into the 0^{th} and 1^{st} order beams.

Actuation of the PZT at the oscillator driving frequency generates acoustic waves within the glass which leads to periodic spatial variations in the glass refractive index due to the changes in density (i.e., a moving diffraction grating is produced). When laser light is incident on the moving diffraction grating, it is diffracted into multiple separate beams (or orders). The diffraction angles, θ, are given by Eq. 1, where m = 0, ±1, ±2, … is the order number, λ is the light wavelength (633 nm), and ν is the acoustic wavelength. Under high driving frequencies and by proper design, a portion of the light is diffracted into the 1^{st} order (m = 1) beam while the rest (0^{th} order beam) passes through the glass; see Fig. 2.

$$\sin\theta = \frac{m\lambda}{2\nu} \tag{1}$$

A photograph and schematic diagram of the AOM DMI setup are provided in Fig. 3. In Fig 3(b), a single frequency laser is used as the light source rather than the two frequency source applied in polarization dependent configurations. The beam passes through the first acousto-optic modulator (AOM1). Setting the angle of AOM1 (f_1 driving frequency) to the incident beam as shown in Eq. 1 produces the 0^{th} order and 1^{st} order beams. The frequency of the 0^{th} order beam is simply the optical frequency, f_o, while the 1^{st} order beam frequency is $f_o + f_1$. The 0^{th} order beam continues toward the second acousto-optic modulator (AOM2), which is driven at frequency f_2, while the 1^{st} order beam is directed toward the fixed retroreflector for the measurement signal and one of the two retroreflectors for the reference signal. The 0^{th} order beam from AOM1 passes through AOM2. The 1^{st} order (diffracted) beam from AOM2 with a frequency of $f_o + f_2$ is directed toward the moving retroreflector and the second retroreflector for the reference signal. Both the 1^{st} order beams from AOM1 and AOM2 are retroreflected and recombined at AOM1 (i.e., it functions essentially as a beamsplitter). The reference and measurement interference signals, with a beat frequency equal to two times the difference between the two AOM (user selected) driving frequencies, are collected using two photodetectors with fiber optic pickups. The reader may note that the angle of 1^{st} order diffracted beam in Fig. 3(b) is exaggerated. Sufficient distance is needed for the beams from the AOMs to be separated and directed onto each retroreflector due to the small diffraction angle from the AOMs (approximately 7 mrad or 0.4 deg).

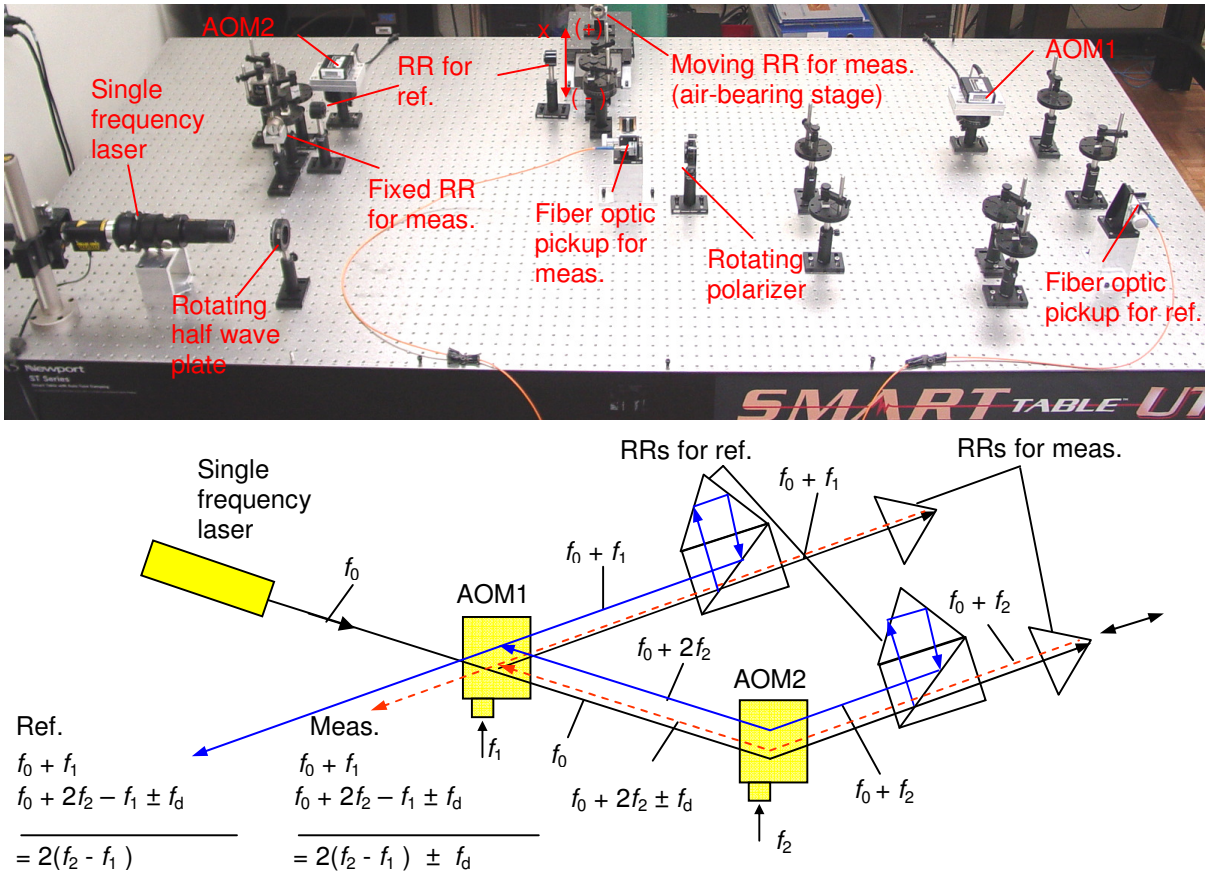

FIGURE 3. (a) Experimental setup of heterodyne interferometer using acousto-optic modulators to spatially separate the beams. (b) Schematic of acousto-optic modulator based interferometer showing the beam separation and combination at each AOM.(RR is used to abbreviate retroreflector.)

EXPERIMENTAL RESULTS

In this section, the frequency content of interference signals from the AOM DMI (collected using a spectrum analyzer) is presented. The undesired interference terms, which cause periodic error, are not observed in the spectrum. Data was collected while the target displaced in the +x direction (see Fig. 3(a)). The beat frequency for a first alignment was 3.64 MHz; it was obtained by setting f_1 to 40 MHz and f_2 to 41.82 MHz. Figures 4 shows the frequency content for the velocities of 10,000 mm/min. The corresponding Doppler shift is 0.53 MHz. It is seen that only the desired *ac interference* signal (3.64 + 0.53) MHz and *dc power* peak are present with no content at the *ac reference* signal (first order periodic error) frequency of 3.64 MHz or the leakage induced *ac interference* signal (second order periodic error) frequency of (3.64 – 0.53) MHz.

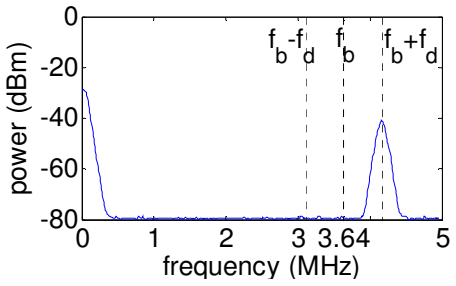

FIGURE 4. Desired ac interference term and dc peak for 10,000 mm/min (f_d = 0.53 MHz). No other content is present.

In Fig. 5(a), spectra for a single target velocity (10,000 mm/min) for various linear polarizer angles are shown. Again, unwanted interference signals are not present for any angular orientation. The test results from a polarization-coded interferometer for the same test conditions are provided in Fig. 5(b) for comparison purposes. It is seen that both first and second order periodic error are present.

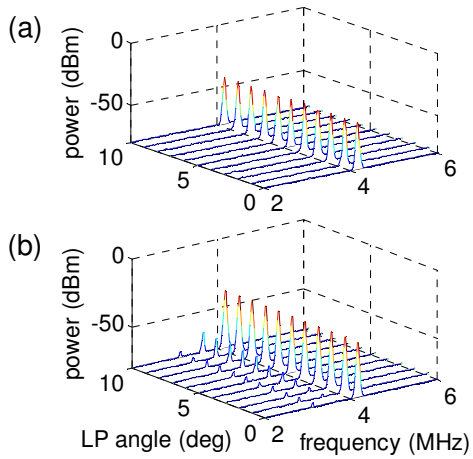

FIGURE 5. (a) No undesired frequency content for the AOM DMI with linear polarizer (LP) angle variation. (b) The leakage induced interference terms accompany the desired ac interference signal for the traditional DMI with the same test setup as the AOM DMI.

One of the advantages in the new design of the interferometer is the ability to tune the beat frequency by adjusting the driving frequency for the two acousto-optic modulators. This makes the new design compatible with existing phase measuring hardware/software independent of the system specific beat frequency. To demonstrate the variable beat frequency capability, the driving frequency for AOM2 was modified to f_2 = 42.5 MHz, while f_1 was maintained at 40 MHz. This gave a new beat frequency of f_b = 5 MHz. Figure 6 shows the spectra for this new configuration at target velocities of 10,000 mm/min. No periodic error content is observed.

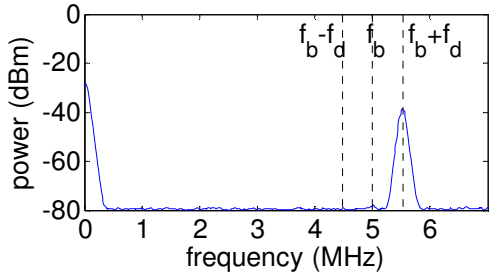

FIGURE 6. Result for new beat frequency of 5 MHz. No periodic error frequency content is observed for target velocity of 10,000 mm/min (f_d = 0.53 MHz).

CONCLUSIONS

This study demonstrated a new displacement measuring interferometer configuration that exhibits no periodic error. Experimental results were presented for two arrangements of the new design, which showed the capability to arbitrarily set the beat frequency. Spectral content was collected using a spectrum analyzer to verify zero periodic error. These results were compared to data obtained from a traditional polarization-coded heterodyne interferometer.

ACKNOWLEGEMENTS

This work was supported by the National Science Foundation (DMI-0555645) and Agilent Technologies, Inc. Any opinions, findings, and conclusions or recommendations expressed in this material are those of the authors and do not necessarily reflect the views of these agencies.

REFERENCES

[1] Quenelle R. Nonlinearity in interferometric measurements. Hewlett-Packard Journal 1983; 34(4):10.

[2] Badami V, Patterson S. A frequency domain method for the measurement of nonlinearity in heterodyne interferometry. Precision Engineering 2000; 24(1):41-49.

[3] Cosijns S, Haitjema H, Schellekens P. Modeling and verifying non-linearities in heterodyne displacement interferometry. Precision Engineering 2002; 26:448-455.

[4] Stone J, Howard L. A simple technique for observing periodic nonlinearities in Michelson interferometers. Precision Engineering 1998; 22(4):220-232.

[5] Patterson S, Beckwith J. Reduction of systematic errors in heterodyne interferometric displacement measurement, In: Proceedings of the 8th International Precision Engineering Seminar (IPES), Compiegne, France, 1995. pp. 101-104.

[6] Tanaka M, Yamagami T, Nakayama K. Linear interpolation of periodic error in a heterodyne laser interferometer at subnanometer levels. IEEE Transactions on Instrumentation and Measurement 1989; 38(2):552-554.

[7] Wu C, Lawall J, Deslattes R. Heterodyne interferometer with subatomic periodic nonlinearity. Applied Optics 1999; 38(19):4089-4094.

[8] Schmitz T, Beckwith J. An investigation of two unexplored periodic error sources in differential-path interferometry. Precision Engineering 2002; 27(3):311-322.